IOP Publishing Phys. Med. Biol. 67 (2022) 065011 https://doi.org/10.1088/1361-6560/ac5a94

Physics in Medicine & Biology

IPEM Institute of Physics and Engineering in Medicine

OPEN ACCESS

RECEIVED
17 October 2021

REVISED
28 January 2022

ACCEPTED FOR PUBLICATION
28 February 2022

PUBLISHED
17 March 2022

PAPER

Determination of beam quality correction factors for the Roos plane-parallel ionisation chamber exposed to very high energy electron (VHEE) beams using Geant4

M McManus[1,2,*], **F Romano**[3], **G Royle**[2], **D Botnariuc**[1,2], **D Shipley**[1], **H Palmans**[1,4] and **A Subiel**[1]

[1] National Physicsal Laboratory, Hampton Road, Teddington, TW11 0LW, United Kingdom
[2] University College London, Gower Street, WC1E 6BT, United Kingdom
[3] Instituto Nazionale Di Fisica Nucleare, Sezione Di Catania, Catania, Italy
[4] MedAustron Ion Therapy Center, Marie-Curie Strasse 5, A-2700 Wiener Neustadt, Austria
[*] Author to whom any correspondence should be addressed.

E-mail: michael.scmcmanus@pm.me **and** anna.subiel@npl.co.uk

Keywords: geant4, Monte Carlo, perturbation factors, beam quality correction, VHEE

Abstract

Detailed characterisation of the Roos secondary standard plane-parallel ionisation chamber has been conducted in a novel 200 MeV Very High Energy Electron (VHEE) beam with reference to the standard 12 MeV electron calibration beam used in our experimental work. Stopping-power-ratios and perturbation factors have been determined for both beams and used to calculated the beam quality correction factor using the Geant4 general purpose MC code. These factors have been calculated for a variety of charged particle transport parameters available in Geant4 which were found to pass the Fano cavity test. Stopping-power-ratios for the 12 MeV electron calibration beam quality were found to agree within uncertainties to that quoted by current dosimetry protocols. Perturbation factors were found to vary by up-to 4% for the calibration beam depending on the parameter configuration, compared with only 0.8% for the VHEE beam. Beam quality correction factors were found to describe an approximately 10% lower dose than would be originally calculated if a beam quality correction were not accounted for. Moreover, results presented here largely resolve unphysical chamber measurements, such as collection efficiencies greater than 100%, and assist in the accurate determination of absorbed dose and ion recombination in secondary standard ionisation chambers.

1. Introduction

The use of Very High Energy Electron (VHEEs), with energies up-to 250 MeV, as a promising future radiotherapy modality has been investigated in detail through Monte Carlo (MC) simulations which have shown increased penetration depth, improved target volume conformity and reduced healthy tissue irradiation and organ-at-risk doses compared to current clinical radiotherapy techniques (DesRosiers *et al* 2000, Bazalova Carter *et al* 2015, Schüler *et al* 2017). Moreover, focusing VHEEs can improve peak doses by more than an order of magnitude compared with the equivalent collimated beam (Kokurewicz *et al* 2019).

Significant challenges have been shown to arise when attempting to conduct absolute dosimetry in a novel high dose-rate VHEE beamline at the CLEAR facility in CERN (McManus *et al* 2020). This beam is a quasi mono-energetic electron source capable of delivering energies up-to 220 MeV (Gamba *et al* 2018). In particular, when using secondary standard ionisation chambers, a large ion recombination effect occurs with as little as 4% of produced charge being collected by the chamber at high dose-per-pulse (McManus *et al* 2020). As there are no VHEE calibration beams, there is no chamber specific calibration coefficient for a VHEE beam quality, $N_{D,w,Q}$, such that the chamber charge measurement can be accurately converted to dose-to-water. It is then necessary to apply a beam quality correction factor, k_{Q,Q_0}, in order to convert from a known calibration beam quality in which the chamber has been previously calibrated, Q_0, to the user beam quality, Q. Use of an incorrect

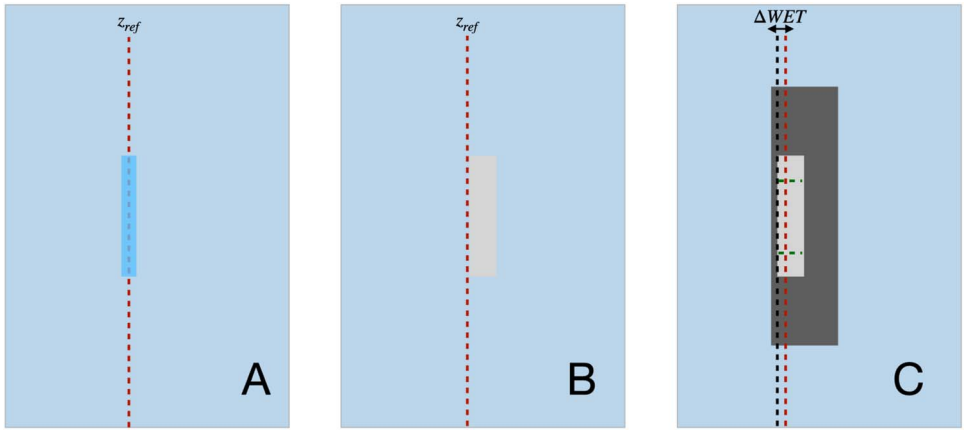

Figure 1. Schematic of the three geometries used to determine ionisation chamber perturbation factors. Plot *A* shows a thin water volume centred at the reference depth in water, plot *B* shows the chamber air cavity positioned with the surface of the cavity at the reference depth in water, and plot *C* shows the full ion chamber geometry positioned such that the front surface of the air cavity is placed at the reference depth in water, accounting for the WET of the chamber entrance window (red dashed line). The scoring volume in plot C is defined within the horizontal green dashed line.

calibration coefficient could lead to an underestimation of the recombination effect or result in un-physical charge measurements where the chamber appears to collect greater than 100% of the produced charge.

The EGSnrc MC code has been chosen repeatedly for calculation of beam quality correction factors, as well as its component perturbation factors and stopping-power-ratios (SPRs), as it claims accuracy in ionisation chamber simulations within 0.1% (Kawrakow 2000). Despite this, EGSnrc is only capable of handling the simulation of electrons, positrons and photons. At the VHEE energy of 200 MeV investigated in this work, there is a probability of secondary heavy particle production such as neutrons and protons. Therefore, the Geant4 general purpose MC code was chosen (Agostinelli *et al* 2003, Allison *et al* 2006, 2016). Perturbation factors for multiple ion chambers have been calculated previously for clinical energy electron beams using EGSnrc (Zink and Wulff 2009, Bailey *et al* 2015), as well as proton beams using FLUKA (Lourenço *et al* 2019) and TOPAS/Geant4 (Wulff *et al* 2018). However, Geant4 has never before been used for the calculation beam quality correction for clinical energy electron or VHEE beams.

This work aims to provide detailed determination of SPRs and perturbation factors for the standard 12 MeV electron calibration beam and the novel 200 MeV VHEE beam used in our experimental work, both of which are required to calculate the subsequent beam quality correction factors using the Geant4 general purpose MC code.

2. Materials and methods

2.1. Theory

The dose-to-water (measured in Gray (Gy)) inferred from an ionisation chamber exposed to the user beam quality, $D_{w,Q,ion}$, is calculated as follows:

$$D_{w,Q,ion} = M_Q N_{D,w,Q_0} k_{Q,Q_0} \tag{1}$$

where M_Q is the charge measured in Coulombs collected in the ionisation chamber at a particular collecting voltage corrected for influence quantities such as polarity, temperature and pressure and ion recombination, and N_{D,w,Q_0} is the calibration coefficient for the calibration beam quality. The theoretical value of the beam quality correction factor, k_{Q,Q_0}, is found through equation (2)

$$k_{Q,Q_0} = \frac{(W/e)_Q}{(W/e)_{Q_0}} \frac{p_Q}{p_{Q_0}} \frac{s^{SA}_{w,a,Q}}{s^{SA}_{w,a,Q_0}}, \tag{2}$$

where $(W/e)_i$ is the average energy required to create an ion pair in air, $_{pi}$ is the perturbation factor of the ion chamber and $s^{SA}_{w,a,i}$ is the Spencer-Attix water(w)-to-air(a) SPR, each with $i = Q, Q_0$. The $(W/e)_i$ values are assumed to be constant with energy and therefore their quotient is taken to be unity. Perturbation factors are dependent on the composition and geometry of the user chamber and beam quality. As one requires dose-to-water, $_{pi}$ accounts for the non water-equivalent components present in ionisation chambers. For plane-parallel chambers, one can split the contribution of $_{pi}$ into two separate calculations, the *wall* perturbation, p_{wall}, and the *air cavity* pertubation, p_{cav}. The formalism of the individual perturbation factors and the SPR is given in equations (3)–(6)

$$p_i = p_{wall,i} \cdot p_{cav,i} \tag{3}$$

$$p_{wall,i} = D_{a,i}/D_{cham,i} \tag{4}$$

$$p_{cav,i} = D_{w,i}/(D_{a,i} \cdot s^{SA}_{w,a,i}) \tag{5}$$

$$s^{SA}_{w,a,i} = \frac{\int_{\Delta}^{E_{\max}} \Phi_{E,w}[L(E,\Delta)/\rho]_w \, dE + \Phi_{\Delta,w}[S(\Delta)/\rho]_w \, \Delta}{\int_{\Delta}^{E_{\max}} \Phi_{E,w}[L(E,\Delta)/\rho]_a \, dE + \Phi_{\Delta,w}[S(\Delta)/\rho]_a \, \Delta}, \tag{6}$$

where $D_{cham,i}$ is the dose to the air cavity of the chamber with all components present including the entrance window and graphite electrodes (figure 1(C)), $D_{a,i}$ is the dose to the chamber air cavity in the absence of all chamber components except the air cavity itself (figure 1(B)), $D_{w,i}$ is the dose to a thin cavity volume of water (figure 1(A)), $\Phi_{E,w}$ is the particle fluence in the thin water volume, differential in energy, $[L(E,\Delta)/\rho]_j$ is the restricted stopping power with energy production threshold, Δ, and $[S(\Delta)/\rho]_j$ is the unrestricted stopping-power for particles of energy equal to the threshold, with $j = w, a$. The terms outside of the integral in equation (6) are referred to as the *track-ends*, which account for energy deposited in the cavity from particles which fall below the threshold energy (Nahum 1978).

Based on detailed MC simulations of multiple clinical electron accelerators, *Burns et al (1996)* were able to determine an empirical formula for the SPR at a given reference depth using the R_{50} beam quality specifier, which is the depth a beam has penetrated once it reaches 50% of its maximum dose deposit (Burns *et al* 1996). This formula is given in equation (7)

$$s^{B}_{w,a,i} = 1.253 - 0.1487(R_{50})^{0.214}, \tag{7}$$

where $s^{B}_{w,a,i}$ denotes the Burns value of the SPR for beam quality i, with uncertainty of 0.2% for electron sources.

Following the recommendations of the TRS-398 code of practice for clinical electron dosimetry, the reference ionisation chamber was enclosed in a water phantom and positioned with respect to an effective point of measurement, P_{eff}, and the reference depth in water, z_{ref} (IAEA 2000). The P_{eff} of a plane-parallel chamber is defined as the depth of the front surface of the air cavity in water, whilst z_{ref} is the depth in water at which P_{eff} of an ionisation chamber should be placed. The reference depth is defined as:

$$z_{ref} = 0.6R_{50} - 0.1 \text{ cm}. \tag{8}$$

2.2. Monte carlo geometry setup

For the MC calculation of $s^{SA}_{w,a,i}$ and $D_{w,i}$, the geometry in figure 1(A) was applied which defines a thin volume of water of thickness 0.02 cm enclosed in a water phantom. The thin water volume is centred at z_{ref} such that the dose-to-water at the reference depth can be determined. The thickness of this volume was chosen to ensure there is minimal or no dose gradient across the volume (Bailey *et al* 2015).

The volume-averaged particle fluence in a MC simulation can be determined from the sum of track lengths per unit volume, $\sum dl/dV$, as described by *Kellerer* (Kellerer 1971). To calculate $\Phi_{E,w}$ in Geant4 10.07-p01, a *Sensitive Detector* class was implemented to score both the dose-per-step and step-size of each step any particle made inside the bounds of the thin water volume. The restricted stopping-power in water, $[L(E,\Delta)/\rho]_w$, was calculated using the midpoint energy of each step through an in-built function available in Geant4. The same midpoint energy was used for the calculation of the restricted stopping-power in air, $[L(E,\Delta)/\rho]_a$.

The dose-to-air, $D_{a,i}$, was scored in an air cavity, representative of the Roos ion chamber sensitive volume with diameter of 1.56 cm, surrounded by water as depicted in figure 1(B). The surface of the air cavity is positioned at z_{ref} as this is where P_{eff} would be within the full chamber geometry. The dose-to-chamber, $D_{cham,i}$, geometry is shown in figure 1(C), whereby the dose to the air cavity is scored within the horizontal dashed lines, defining the sensitive volume diameter of 1.56 cm. The air outside of the sensitive volume is known as the chamber guard ring. As z_{ref} refers to a depth in water, the position of the chamber geometry must be adjusted to account for the water-equivalent-thickness (WET) of the chamber's entrance window. For the Roos chamber, the entrance window is composed of 1.11 mm of PMMA with density of 1.19 g cm^{-3} and 0.02 mm of graphite with density 0.82 g cm^{-3}. The WET of the Roos chamber entrance window up-to the effective point of measurement was calculated to be approximately 1.283 mm. Therefore, to ensure that P_{eff} is positioned at z_{ref} the chamber was moved towards the source by a distance equal to the difference between the WET and the physical thickness of the chamber, $\Delta WET = 0.0153$ cm. This updated position is represented by the red dashed line in figure 1(C). The new position of z_{ref} is shown by the black dashed line of figure 1(C). Moreover, to ensure that the physical distance between the source and P_{eff} was unchanged between geometry setups, the source exposing figure 1(C) was also moved a further 0.0153 cm from the surface of the phantom.

A 12 MeV clinical electron beam at the National Physical Laboratory (NPL) was used as the calibration beam quality as the Roos chamber described in this study had been cross calibrated against a secondary standard ion chamber in this beam at the NPL. As described by TRS-398 for reference dosimetry using electrons, a 20 × 20

cm^2 source field was placed 100 cm from the surface of the water phantom with dimensions of $100 \times 100 \times 30$ cm^3. An output energy-fluence spectrum of the NPL accelerator, determined using EGSnrc by Bailey *et al* (2015) was implemented as input to the Geant4 simulation, where the mean energy of the beam was approximately 11.8 MeV (Bailey *et al* 2015).

For the 200 MeV user beam, the MC source was setup as close as possible to the experimental beam conditions (McManus *et al* 2020). This included a circular source field of size 5 mm σ in both x and y, and a Gaussian energy distribution with 0.425 MeV σ. Again, in an attempt to follow the current dosimetry protocols, the source was placed 100 cm from the surface of a water phantom of dimensions $100 \times 100 \times 50$ cm^3.

Generally, the threshold energy in equation (6) is taken as the minimum energy required by an electron to cross the air cavity of a chamber. In the case of the PTW Roos chamber investigated in this work, with a cavity width of 2 mm, the threshold corresponds to an energy of approximately $\Delta = 10$ keV in air. In Geant4, this energy threshold was achieved for all materials by reducing the so-called *Range Cut* to 6.1 μm i.e. particles with a CSDA range less than this value will not produce secondary particles. Moreover, a lower limit of 10 keV was set in the *Production Cuts table* in Geant4. As it is not possible to explicitly set a production threshold in terms of energy in Geant4, both the application of a *Range Cut* and a lower limit on the *Production Cuts* are necessary to force a secondary particle production threshold of $\Delta = 10$ keV across the entire simulation. To improve simulation performance, these production cuts were only applied to the chamber and cavity volumes, and a virtual water volume surrounding them in order to account for any backscattering. In the 12 MeV case, this surrounding volume was set to $6 \times 6 \times 4$ cm^3, and in the 200 MeV case $6 \times 6 \times 6$ cm^3. Outside of these volumes, the range cut was set to the Geant4 default of 1 mm.

2.3. Monte carlo physics implementation

All simulations in this study were conducted using the Geant4 10.07-p01 general purpose MC code. The physics lists used were the *G4EMStandardPhysics-Option4* electro-magnetic physics, with the *QBBC* reference nuclear physics list (recommended for medical applications) included in the 200 MeV case to account for inelastic nuclear interactions where larger charged particle such as protons could be produced (Geant4 Collaboration 2020). Material definitions were made using the NIST material database available in Geant4 with the exception of the graphite electrodes which were set manually due to their unique density. Moreover, ICRU90 excitation energy data was used (Seltzer *et al* 2016).

This study distinguished various charged particle transport parameter configurations available in Geant4 which passed a Fano test conducted previously by McManus *et al* (2021) and, therefore, should provide accurate ion chamber simulation results (McManus *et al* 2021). Transport parameters modified included the *Range Factor*, f_r, and *Geometry Factor*, f_g, which both affect the initial step size of a particle in a new volume, the *skin* parameter which controls the amount of single scattering which is employed around a boundary, and the fractional step size reduction per step as a particle approaches a boundary, dR/R. Default values for these parameters are $f_r = 0.08$, $f_g = 2.5$, $skin = 3$ and $dR/R = 0.2$. In this study, when a particular parameter is defined, e.g. $f_r = 0.01$, all other parameters are at their default value.

For a detailed discussion of the Fano test implementation and results, please refer to the study of *McManus et al* (2021) (McManus *et al* 2021).

Once physics transport parameter configurations were established which passed the Fano test, depth-dose simulations were performed and the R_{50} and subsequent z_{ref} values were determined for each set of parameter configurations. For the depth-dose calculations, the bin resolution was set to 0.05 cm and a quadratic interpolation of the curve was used to determine the MC reference depth. For the 12 MeV case, 10^9 histories were simulated and achieved a statistical uncertainty below 0.2%, whereas in the 200 MeV case, only 5×10^7 histories were simulated to achieve a statistical uncertainty below 0.1%.

3. Results

3.1. Perturbation factors

The depth-dose curve for the 12 MeV calibration beam with all default EM option-4 physics parameters is shown in figure 2. The MC reference depth was calculated to be $z_{ref,MC} = 2.75$ cm. The experimentally determined reference depth in water of the NPL clinical electron beam was found to be $z_{ref,m} = 2.74$ cm. Varying the charged particle transport parameters yielded different values of $z_{ref,MC}$ ranging from 2.744 cm for $f_r = 0.001$ to 2.760 cm for $skin = 1$. Subsequently, the value of s^{SA}_{w,a,Q_0} also varied between 1.041 at $f_r = 0.001$ and 1.044 for the majority of the other transport parameter configurations, with a relative uncertainty of 0.003%. The wall perturbation, $p_{wall,Q_0,MC}$, varied between 0.9983 and 1.0269 with a relative uncertainty of 0.13%. The cavity perturbation factor, $p_{cav,Q_0,MC}$, showed variation between 0.9697 and 1.0064 with a relative uncertainty of 0.12%. Finally, the total value of perturbation, $p_{Q_0,MC}$, varied from 0.9809 to 1.0177 with a relative uncertainty of 0.18%.

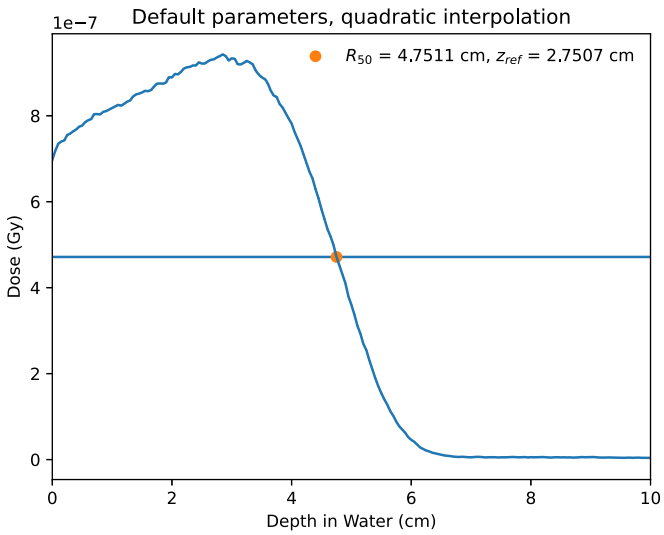

Figure 2. Depth-dose curve of the 12 MeV calibration beam with all default MC transport parameters. The source was composed of a 20×20 cm^2 field placed 100 cm from the surface of the water phantom, and the dose was scored in a cylinder of diameter 1.56 cm, equivalent to the sensitive volume of the Roos ionisation chamber, and length of 10 cm.

Table 1. Stopping-power-ratios and perturbation factors for the 12 MeV beam using the MC calculated reference depth, $z_{ref,MC}$, with their relative uncertainty given in brackets at a $k = 1$ coverage level. Each transport parameter was modified individually.

	12 MeV perturbation factors with $z_{ref,MC}$					
Transport parameter	$z_{ref,MC}$ (cm)	s^{B}_{w,a,Q_0} ($\pm$0.2%)	$s^{SA}_{w,a,Q_0,MC}$ ($\approx \pm$ 0.003%)	$p_{wall,Q_0,MC}$ ($\approx \pm$ 0.13%)	$p_{cav,Q_0,MC}$ ($\approx \pm$ 0.12%)	$p_{Q_0,MC}$ ($\approx \pm$ 0.18%)
Default	2.75068	1.045	1.044	0.9983	0.9980	0.9963
$f_r = 0.01$	2.750 66	1.045	1.044	0.9960	1.000 06	0.9961
$f_r = 0.005$	2.753 96	1.045	1.044	0.9907	0.9984	0.9892
$f_r = 0.0025$	2.754 97	1.045	1.043	0.9945	1.0005	0.9950
$f_r = 0.001$	2.743 93	1.046	1.041	0.9963	1.0044	1.0007
$f_g = 3$	2.749 33	1.045	1.044	1.0269	0.9697	0.9957
skin = 1	2.760 25	1.045	1.044	1.0090	0.9904	0.9993
skin = 5	2.748 29	1.045	1.044	1.0012	1.0013	1.0024
$dR/R = 0.4$	2.753 48	1.045	1.044	1.0255	0.9924	1.0177
$dR/R = 0.8$	2.752 51	1.045	1.044	1.0068	0.9743	0.9809
$dR/R = 1$	2.754 32	1.045	1.044	1.0099	1.0064	1.0164

All values of perturbation factors and SPRs with the MC calculated reference depth can be seen in table 1, with the relative uncertainty quoted as the Type-A statistical uncertainty from the MC simulation at a $k = 1$ coverage factor.

For the experimentally determined reference depth, $z_{ref,m} = 2.74$ cm, the value of $s^{SA}_{w,a,Q_0,m}$ was again found to decrease with decreasing f_r, with the associated uncertainty also decreasing from 0.0034% at $f_r = 0.08$ to 0.0025% at $f_r = 0.001$. The wall perturbation was found to vary from 0.9844 to 1.0307 with a relative uncertainty of 0.15%. A significant cavity perturbation was found at $f_r = 0.01$ of 0.9573, with values increasing to 1.0187 at $f_g = 3$ with a relative uncertainty of 0.12%. The total perturbation at $z_{ref,m}$, $p_{Q_0,m}$, was found to vary from 0.9749 to 1.0178 with a relative uncertainty of 0.18%. All perturbation factors and SPRs at $z_{ref,m}$ can be found in table 2.

The depth-dose curve for the 200 MeV user beam is shown in figure 3 with all default transport parameters and nuclear interactions included. As the VHEE beam described is not a broad beam, it is improper to define a reference depth based on this source as it was not determined under reference conditions. However, for simplicity, the depth in MC used for all calculations is still referred to as a z_{ref}. The calculated depth in MC was found to be $z_{ref,MC,n} = 12.74$ cm. As no measured reference depth for VHEEs under reference conditions exists, the SPRs and perturbation factors have been compared with and without nuclear interactions included, identified with the additional *n* (nuclear) and *nn* (no-nuclear) indices, respectively.

The estimated SPR based on the Burns equation, given an R_{50} representative of a 200 MeV source, was $s^{B}_{w,a,Q} = 0.967 \pm 0.2\%$. This value is, however, unlikely to be accurate given that the Burns equation was determined for reference beams with broad field sizes. The values of $s^{SA}_{w,a,Q,n}$ and $s^{SA}_{w,a,Q,nn}$ ranged from 0.9002 to

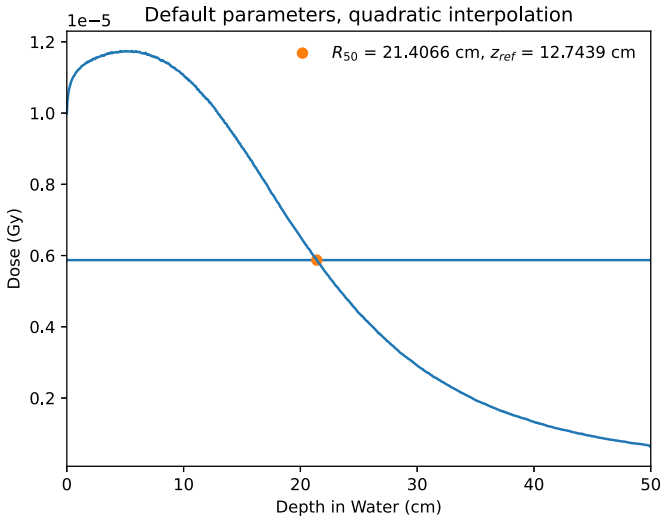

Figure 3. Depth-dose curve of the 200 MeV user beam with all default MC transport parameters and 175 MeV MSC boundary energy. The source was composed of a 5 mm σ $x - y$ field placed 100 cm from the surface of the water phantom, and the dose was scored in a cylinder of diameter 1.56 cm and length of 50 cm.

Table 2. Stopping-power-ratios and perturbation factors for the 12 MeV beam using the measured reference depth, $z_{ref,m}$, with the relative uncertainty shown in brackets at a $k = 1$ coverage level. Each parameter was modified individually.

	12 MeV perturbation factors with $z_{ref,m}$					
Transport parameter	$z_{ref,m}$ (cm)	s^{B}_{w,a,Q_0} ($\pm$0.2%)	$s^{SA}_{w,a,Q_0,m}$ ($\approx \pm$ 0.003%)	$P_{wall,Q_0,m}$ ($\approx \pm$ 0.15%)	$P_{cav,Q_0,m}$ ($\approx \pm$ 0.12%)	$P_{Q_0,m}$ ($\approx \pm$ 0.18%)
Default	2.74	1.046	1.045	0.9890	1.0164	1.0053
$f_r = 0.01$	2.74	1.046	1.044	1.0234	0.9573	0.9797
$f_r = 0.005$	2.74	1.046	1.043	0.9856	0.9892	0.9749
$f_r = 0.0025$	2.74	1.046	1.042	1.0018	0.9974	0.9992
$f_r = 0.001$	2.74	1.046	1.041	1.0089	0.9796	0.9884
$f_g = 3$	2.74	1.046	1.045	0.9844	1.0187	1.0028
$skin = 1$	2.74	1.046	1.044	0.9994	0.9803	0.9798
$skin = 5$	2.74	1.046	1.044	1.0084	0.9767	0.9849
$dR/R = 0.4$	2.74	1.046	1.044	0.9939	0.9988	0.9927
$dR/R = 0.8$	2.74	1.046	1.044	1.0307	0.9875	1.0178
$dR/R = 1$	2.74	1.046	1.043	1.0049	1.0028	1.0078

0.9026 with a relative uncertainty of approximately 0.003%, which was not obviously affected by the inclusion of nuclear interactions. All perturbation factors and SPRs at 200 MeV with nuclear interactions included can be seen in table 3 with their associated relative uncertainty quoted as Type-A with a coverage factor of $k = 1$.

With the exception of $skin = 5$ and $dR/R = 0.4$, the removal of nuclear interactions resulted in larger values of $p_{wall,Q,nn}$ in comparison to $p_{wall,Q,n}$. In contrast, the resulting $p_{Q,nn}$ was found to be marginally larger, in some cases simply within uncertainties, than $p_{Q,n}$, with the exception of $f_r = 0.0025$ and $dR/R = 0.4$. All perturbation factors were found to remain stable at 200 MeV regardless of parameter configuration with a maximum variation of only 0.4% for both $p_{wall,Q,n}$ and $p_{wall,Q,nn}$, 0.5% for $p_{cav,Q,nn}$ and 0.6% for $p_{cav,Q,n}$, and 0.7% for $p_{Q,n}$ and 0.5% for $p_{Q,nn}$. All perturbation factors and SPRs at 200 MeV without nuclear interactions can be seen in table 4 with their associated relative uncertainty quoted as Type-A with a coverage factor of $k = 1$.

3.2. Beam quality correction

Following the evaluation of the perturbation factors, the corresponding k_{Q,Q_0} values were determined for the passing parameter configurations common to all beams i.e. 12 MeV with measured and MC reference depths and 200 MeV with and without nuclear interactions. These parameters were $f_r = 0.01, 0.0025$, $f_g = 3$, $skin = 5$ and $dR/R = 0.4$. The beam quality correction factor using nuclear interactions has been given by $k_{Q,n,Q_0,m}$ and $k_{Q,n,Q_0,MC}$ for Q_0 with the measured and MC reference depths, respectively. Similarly, without nuclear interactions is given by $k_{Q,nn,Q_0,m}$ and $k_{Q,nn,Q_0,MC}$ for Q_0 with measured and MC reference depths, respectively. Each value of beam quality correction factor can be seen in table 5. The largest correction in beam quality was

Table 3. Stopping-power-ratios and perturbation factors for the 200 MeV beam including nuclear interactions. Relative uncertainties are shown in brackets at a $k = 1$ coverage level. Each parameter was modified individually.

200 MeV perturbation factors with $z_{ref,MC}$–nuclear interactions included						
Transport parameter	$z_{ref,MC,n}$ (cm)	$s^{B}_{w,a,Q}$ (±0.2%)	$s^{SA}_{w,a,Q,n}$ (± ≈ 0.003%)	$p_{wall,Q,n}$ (± ≈ 0.055%)	$p_{cav,Q,n}$ (± ≈ 0.045%)	$p_{Q,n}$ (± ≈ 0.070%)
Default	12.7439	0.967	0.9026	1.0014	1.0449	1.0463
$f_r = 0.01$	12.7295	0.967	0.9025	1.0012	1.0466	1.0479
$f_r = 0.005$	12.7405	0.967	0.9017	1.0026	1.0461	1.0488
$f_r = 0.0025$	12.7300	0.967	0.9002	1.0012	1.0502	1.0515
$f_g = 1$	12.7401	0.967	0.9024	0.9988	1.0452	1.0439
$f_g = 2$	12.7413	0.967	0.9025	1.0002	1.0442	1.0444
$f_g = 3$	12.7421	0.967	0.9025	1.0006	1.0454	1.0461
skin = 1	12.7313	0.967	0.9026	1.0008	1.0451	1.0459
skin = 4	12.7321	0.967	0.9025	1.0005	1.0454	1.0460
skin = 5	12.7250	0.967	0.9026	0.9988	1.0454	1.0441
$dR/R = 0.1$	12.7582	0.966	0.9026	1.0006	1.0443	1.0449
$dR/R = 0.4$	12.7250	0.967	0.9025	1.0026	1.0442	1.0470

Table 4. Stopping-power-ratios and perturbation factors for the 200 MeV beam without nuclear interactions. Relative uncertainties are shown in brackets at a $k = 1$ coverage level. Each parameter was modified individually.

200 MeV perturbation factors with $z_{ref,MC}$–no nuclear interactions						
Transport parameter	$z_{ref,MC,nn}$ (cm)	$s^{B}_{w,a,Q}$ (±0.2%)	$s^{SA}_{w,a,Q,nn}$ (± ≈ 0.003%)	$p_{wall,Q,nn}$ (± ≈ 0.055%)	$p_{cav,Q,nn}$ (± ≈ 0.045%)	$p_{Q,nn}$ (± ≈ 0.070%)
$f_r = 0.01$	12.7397	0.967	0.9025	1.0029	1.0476	1.0506
$f_r = 0.0025$	12.7280	0.967	0.9003	1.0008	1.0497	1.0505
$f_g = 1$	12.7418	0.967	0.9025	1.0018	1.0454	1.0472
$f_g = 3$	12.7435	0.967	0.9026	1.0029	1.0447	1.0477
skin = 4	12.7310	0.967	0.9025	1.0024	1.0447	1.0471
skin = 5	12.7210	0.967	0.9024	1.0002	1.0451	1.0454
$dR/R = 0.1$	12.7585	0.966	0.9026	1.0009	1.0446	1.0455
$dR/R = 0.4$	12.7297	0.967	0.9024	0.9987	1.0463	1.0449
$dR/R = 0.8$	12.7370	0.967	0.9021	1.0006	1.0445	1.0451

Table 5. Beam quality correction factors for each transport parameter for the 200 MeV beam with reference to the 12 MeV calibration beam quality.

Transport parameter	$k_{Q,n,Q_0,m}$	$k_{Q,n,Q_0,MC}$	$k_{Q,nn,Q_0,m}$	$k_{Q,nn,Q_0,MC}$
$f_r = 0.01$	0.9246	0.9074	0.9270	0.9118
$f_r = 0.0025$	0.9091	0.9121	0.9084	0.9113
$f_g = 3$	0.9009	0.9082	0.9024	0.9097
skin = 5	0.9165	0.9005	0.9175	0.9014
$dR/R = 0.4$	0.9117	0.8894	0.9098	0.8875

found to be $k_{Q,n,Q_0,MC} = 0.8894$ and $k_{Q,nn,Q_0,MC} = 0.8875$, using the parameter $dR/R = 0.4$. In contrast, the minimum correction was found to be $k_{Q,n,Q_0,m} = 0.9246$ and $k_{Q,nn,Q_0,m} = 0.9270$, using the parameter $f_r = 0.01$. The relative uncertainty associated with the beam quality correction values was found to be approximately 0.18% at a $k = 1$ coverage level.

4. Discussion and conclusion

A detailed determination of perturbation factors, SPRs and beam quality correction factors applicable to VHEEs with energy of 200 MeV has been conducted using the Geant4 general purpose MC code. Choice of charged particle transport parameter and use of either the MC or measured z_{ref} has been shown to affect the final value of the beam quality correction factor by more than 2%. The inclusion of nuclear interactions has been shown not to affect significantly the final value of k_{Q,Q_0}, with deviations of no more than 0.5%. It is clear that in ionisation

chamber calculations exposed to VHEEs, nuclear interactions result in negligible deviation in k_{Q,Q_0}, however, care must be taken in the choice of z_{ref}.

For the calibration 12 MeV beam quality, SPRs were found to remain largely unchanged at values around 1.044 regardless of transport parameter choice, and in most cases, within uncertainties of the estimated value calculated using equation (7). The reference depth calculated at with $f_r = 0.001$ was found to be $z_{ref,MC} = 2.744$ and is the closest value to the experimentally determined reference depth of any of the transport parameter configurations. A study by Bailey *et al* (2015) showed that the cavity perturbation remains constant within 0.1% despite varying z_{ref}, and indicates that for an electron beam quality of 12 MeV, cavity perturbation is close to negligible and p_{cav} should take a value within 0.1% of unity. In this study, however, p_{cav} was shown to vary, with only $f_r = 0.01, 0.0025$ and $skin = 5$ returning values within approximately 0.1% of unity. Considering p_{cav} using the measured reference depth, no values are within 0.1% of unity. Again, Bailey *et al* (2015) showed that p_{wall} took a value of approximately 1.006 for a Roos cavity exposed to a 12 MeV electron beam quality. Here, $skin = 1$, $dR/R = 0.8$ and $dR/R = 1$ are within approximately 0.3% of this value when using the MC reference depth. When using the measured reference depth, only $dR/R = 1$ and $f_r = 0.001$ returned values within 0.3% of that found by Bailey.

For the 200 MeV electron beam quality, the SPR was found to take a value of approximately 0.90 for all parameter configurations, which indicates that $D_{a,Q}$ is around 10% larger than $D_{w,Q}$. As such, the primary source of perturbation at 200 MeV came from the cavity, with more than 4.4% perturbation for all parameter configurations compared with a maximum wall perturbation of only 0.29% at $f_g = 3$ with no nuclear interactions. Given the small thickness of the chamber wall and that the wall material and water have similar densities, the close to negligible p_{wall}, when compared to p_{cav}, appeared justified. The small field size of the 200 MeV beam is likely a contributing factor to the finding that the perturbation factor deviates more from unity compared to the 12 MeV beam. In small photon fields of sizes below 1×1 cm^2, it has been demonstrated that the perturbation of a finite-sized detector is, apart from the volume averaging effect, dominated by the difference in density between the detector medium and water (Cervantes *et al* 2021). This concept has, for example, been discussed at great length by *Bouchard et al (2015)* (Bouchard *et al* 2015a, 2015b). In VHEE's however, it is not clear if this will also be the case since the primary particles are electrons, the knock-on electron spectrum will be very different from the electron recoil spectrum in photons, the energy range of electrons is substantially different and the scatter conditions will be very different. A systematic study of the main influences on the correction factors would be required.

The subsequent value of k_{Q,Q_0} was calculated to be as low as 0.8875 when considering the MC reference depth and no nuclear interactions for $dR/R = 0.4$. This describes a greater than 11% lower dose compared to what would be calculated using the reference calibration coefficient N_{D,w,Q_0} for the VHEE beam quality.

This 200 MeV VHEE beam has also been studied previously by *Poppinga et al (2021)* for the Advanced Markus chamber. In their work, the beam quality correction factor was found to be $k_{Q,Q_0} = 0.79$, however, this was while using Co^{60} as Q_0 beam quality and at a depth of 72 mm in water such that it did not interfere with film measurements (Poppinga *et al* 2020).

As a chamber is calibrated at an experimentally determined reference depth, it is likely that the k_{Q,Q_0} values calculated using $z_{ref,Q_0,m}$ will be most relevant for application in dose calculations.

Finally, considering the VHEE study conducted by (McManus *et al* 2020), several values of the absolute recombination factor were reported to be less than unity, which is an un-physical observation (McManus *et al* 2020). If the authors were to include an updated value of k_{Q,Q_0} determined here, this issue would be largely alleviated and a more accurate and realistic determination of absorbed dose and absolute recombination could be made. For example, the above study quotes a un-physical recombination factor of $k_s = 0.98$ at a 200 V collecting voltage exposed to a clinical dose-per-pulse and using a basic estimated calibration coefficient. Given that a reference depth is typically determined through experiment and not through MC, it is likely that the measured z_{ref} is more applicable. Applying $k_{Q,n,Q_0,m}$, say with $skin = 5$ (0.9165), the new value of recombination would become $k_s = 1.06$. This is a much more realistic value for this dose-per-pulse and collecting voltage. Given that it is extremely difficult to recommend a particular configuration and k_{Q,Q_0} value, one solution may be to take an average of the above values in table 5. For $k_{Q,n,Q_0,m}$, this would provide an average value of approximately 0.9 with a relative uncertainty of 0.4%, giving future dose calculations some degree of confidence. It is clear from this that detailed characterisations of secondary standard ionisation chambers such as this are instrumental in the translation of VHEEs into the clinical setting.

Acknowledgments

This project 18HLT04 UHDpulse has received funding from the EMPIR programme co-financed by the Participating States and from the European Union's Horizon 2020 research and innovation programme.The

authors acknowledge the use of the UCL Myriad High Performance Computing Cluster which facilitated the completion of this work.

ORCID iDs

M McManus https://orcid.org/0000-0003-2538-0874
A Subiel https://orcid.org/0000-0002-3467-4631

References

Agostinelli S *et al* 2003 Geant4a simulation toolkit *Nucl. Instrum. Methods Phys. Res.* A **506** 250–303
Allison J *et al* 2006 Geant4 developments and applications *IEEE Trans. Nucl. Sci.* **53** 270–8
Allison J *et al* 2016 Recent developments in Geant4 *Nucl. Instrum. Methods Phys. Res.* A **835** 186–225
Bailey M, Shipley D R and Manning J W 2015 Roos and NACP-02 ion chamber perturbations and water-air stopping-power ratios for clinical electron beams for energies from 4 to 22 MeV *Phys. Med. Biol.* **60** 1087–105
Bazalova Carter M *et al* 2015 Comparison of film measurements and Monte Carlo simulations of dose delivered with very high-energy electron beams in a polystyrene phantom *Med. Phys.* **42** 1606–13
Bouchard H, Kamio Y, Palmans H, Seuntjens J and Duane S 2015b Detector dose response in megavoltage small photon beams: II. Pencil beam perturbation effects *Med. Phys.* **42** 6048–61
Bouchard H, Seuntjens J, Duane S, Kamio Y and Palmans H 2015a Detector dose response in megavoltage small photon beams: I. Theoretical concepts *Med. Phys.* **42** 6033–47
Burns D T, Ding G X and Rogers D W O 1996 R50 as a beam quality specifier for selecting stopping-power ratios and reference depths for electron dosimetry *Med. Phys.* **23** 383–8
Cervantes Y, Duchaine J, Billas I, Duane S and Bouchard H 2021 Monte Carlo calculation of detector perturbation and quality correction factors in a 1.5 T magnetic resonance guided radiation therapy small photon beams *Phys. Med. Biol.* **66** 225004
DesRosiers C, Moskvin V, Bielajew A F and Papiez L 2000 150–250 MeV electron beams in radiation therapy *Phys. Med. Biol.* **45** 1781
Gamba D *et al* 2018 The CLEAR user facility at CERN *Nucl. Instrum. Methods Phys. Res.* A **909** 480–3
Geant4 Collaboration 2020 Physics Reference Manual, Release 10.7, Rev5.0
IAEA 2000 *Absorbed Dose Determination in External Beam Radiotherapy, Technical Reports Series No. 398* (Vienna: IAEA)
Kawrakow I 2000 Accurate condensed history Monte Carlo simulation of electron transport: II. Application to ion chamber response simulations *Med. Phys.* **27** 499–513
Kellerer A M 1971 Considerations on the random traversal of convex bodies and solutions for general cylinders *Radiat. Res.* **47** 359–76
Kokurewicz K *et al* 2019 Focused very high-energy electron beams as a novel radiotherapy modality for producing high-dose volumetric elements *Sci. Rep.* **9** 10837
Lourenço A, Bouchard H, Galer S, Royle G and Palmans H 2019 The influence of nuclear interactions on ionization chamber perturbation factors in proton beams: FLUKA simulations supported by a Fano test *Med. Phys.* **46** 885–91
McManus M, Romano F, Lee N D, Farabolini W, Gilardi A, Royle G, Palmans H and Subiel A 2020 The challenge of ionisation chamber dosimetry in ultra-short pulsed high dose-rate Very High Energy Electron beams *Sci. Rep.* **10** 1–11
McManus M, Romano F, Royle G, Palmans H and Subiel A 2021 A Geant4 Fano test for novel very high energy electron beams *Phys. Med. Biol.* **66** 245023
Nahum A E 1978 Water/air mass stopping power ratios for megavoltage photon and electron beams *Phys. Med. Biol.* **23** 24
Poppinga D, Kranzer R, Farabolini W, Gilardi A, Corsini R, Wyrwoll V, Looe H K, Delfs B, Gabrisch L and Poppe B 2020 VHEE beam dosimetry at CERN Linear Electron Accelerator for Research under ultra-high dose rate conditions *Biomed. Phys. Eng. Express* **7** 015012
Schüler E, Eriksson K, Hynning E, Hancock S L, Hiniker S M, Bazalova-Carter M, Wong T, Le Q-T, Loo B W and Maxim P G 2017 Very high-energy electron (VHEE) beams in radiation therapy; Treatment plan comparison between VHEE, VMAT, and PPBS *Med. Phys.* **44** 2544–55
Seltzer S M, Fernandez-Varea J M, Andreo P, Bergstrom P M, Burns D T, Krajcar Bronic I, Ross C K and Salvat F 2016 Key Data for ionizing-radiation dosimetry: measurement standards and applications, ICRU Report 90 *Technical Report* (Oxford: Oxford University Press)
Wulff J, Baumann K-S, Verbeek N, Bäumer C, Timmermann B and Zink K 2018 TOPAS/Geant4 configuration for ionization chamber calculations in proton beams *Phys. Med. Biol.* **63** 115013
Zink K and Wulff J 2009 Positioning of a plane-parallel ionization chamber in clinical electron beams and the impact on perturbation factors *Phys. Med. Biol.* **54** 2421–35